CHAPTER 8

HARDWARE IMPLEMENTATION

8.1 INTRODUCTION

In this chapter, the experimental results for the proposed circuits in chapter 4 are given. All the proposed circuits are tested for waveform generation on a laboratory breadboard by using a prototype OTRA circuit. The prototype OTRA circuit is designed by using two AD 844 AN ICs [45-49]. The IC AD 844 AN is a high speed monolithic current feed-back operational amplifier (CFOA). This IC is used in many applications and it can be used in place of traditional op-amps to get much better AC performance and high linearity. The AD 844 AN is very popular by its applications in current-mode circuits. By using this IC many active current-mode devices can be implemented on a laboratory breadboard like second generation current conveyor (CCII), operational transconductance amplifier (OTA), current differencing buffered amplifier (CDBA), current differencing transconductance amplifier (CDTA) and second generation differential current conveyor (DCCII).

The main advantages of using AD 844 AN in current-mode applications, the closed-loop bandwidth is independent of the closed-loop gain and free from the slew rate limitations. To investigate the proposed circuits for waveform generation and frequency tuning with respect to the passive components connected to the circuits, the equivalent prototype circuit model of the OTRA shown in Fig. 2.14 with two AD 844 AN ICs is used. For the OTRA prototype circuit ± 5 V supply voltages are used to produce the oscillations in all the proposed circuits in chapter 4.

8.2 GROUNDED RESISTANCE/CAPACITANCE SINUSOIDAL OSCILLATORS

8.2.1 EXPERIMENTAL RESULTS

The circuits shown in Fig. 4.3 and 4.4 are generated from the generalized configuration shown in Fig. 4.2. These circuits' passive components are connected externally to the inverting and non-inverting terminal of the equivalent circuit model of OTRA shown in Fig. 8.1 on a laboratory breadboard. For the first proposed

minimum component oscillator circuit shown in Fig. 4.3, the passive components R_1 = 10 Ω, R_3 = 1 kΩ, C_2 = 10 nF and C_4 = 1 nF have been used to generate the oscillation.

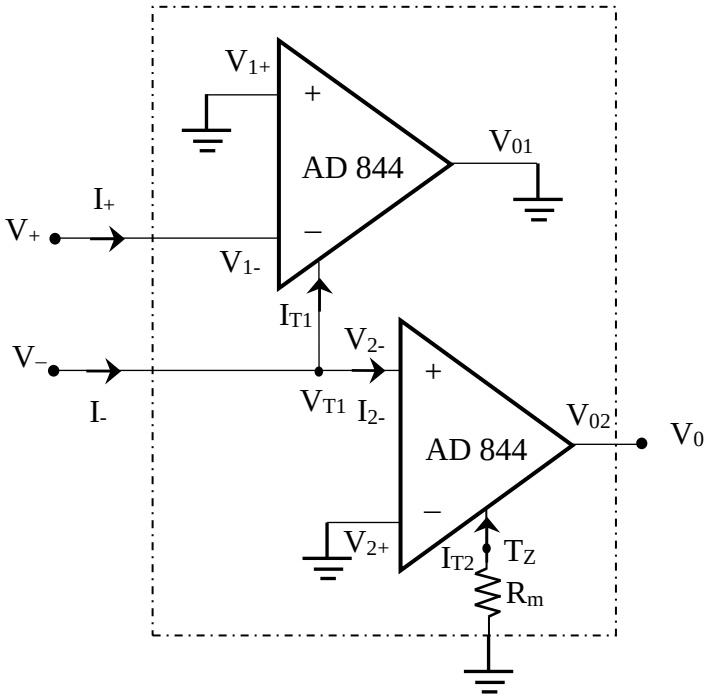

Fig. 8.1 Implementation of OTRA using AD 844 ICs

The corresponding output waveform of the proposed oscillator circuit is shown in Fig. 8.2. The experimental oscillation frequency of the oscillator circuit in Fig. 4.3 is 15.3 kHz, which is close to the theoretical value of 15.9 kHz.

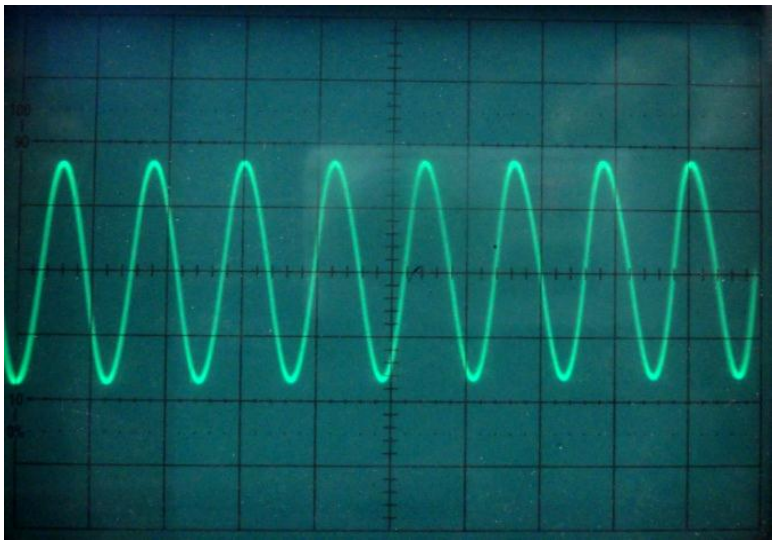

Scale: X-axis 50 μs/div and Y-axis 1 V/div.

Fig. 8.2 Experimental output waveform of the proposed circuit shown in Fig. 4.3

A typical waveform from the oscilloscope screen for the proposed circuit in Fig. 4.4 (a) is presented in Fig. 8.3, which have been obtained for the passive components R_3 = 60 Ω, R_5 = 1 kΩ, R_7 = 300 Ω, C_2 = 10 nF and C_4 = 100 nF. The measured frequency of 22.2 kHz, as shown in Fig. 8.3, which is close to the theoretical result of 22.45 kHz. The percentage of error between the theoretical and practical oscillation frequency is 1.02 %.

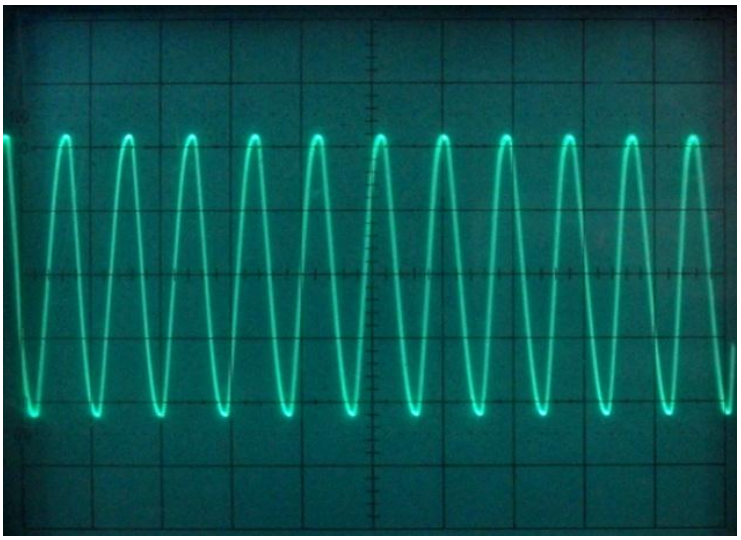

Scale: X-axis 50 µs/div and Y-axis 1 V/div.
Fig. 8.3 Output waveform of the proposed circuit in Fig. 4.4 (a)

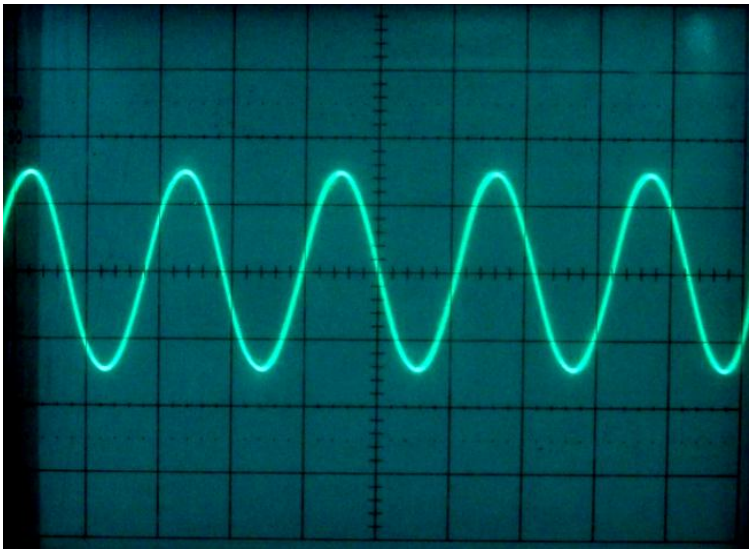

Scale: X-axis 50 µs/div and Y-axis 1 V/div.
Fig. 8.4 Output waveform of the proposed circuit in Fig. 4.4 (b)

The proposed oscillator circuit shown in Fig. 4.4 (b), is designed with the passive components C_1 = 100 nF, C_4 = 100 nF, C_7 = 100 nF, R_3 = 150 Ω and R_5 = 500

Ω on a laboratory breadboard. Figure 8.4 represents the output waveform of the proposed circuit shown in Fig. 4.4 (b). From Fig. 8.4, the oscillation frequency of the second proposed oscillator circuit stands at 5 kHz, which is close to the theoretical value of 5.78 kHz.

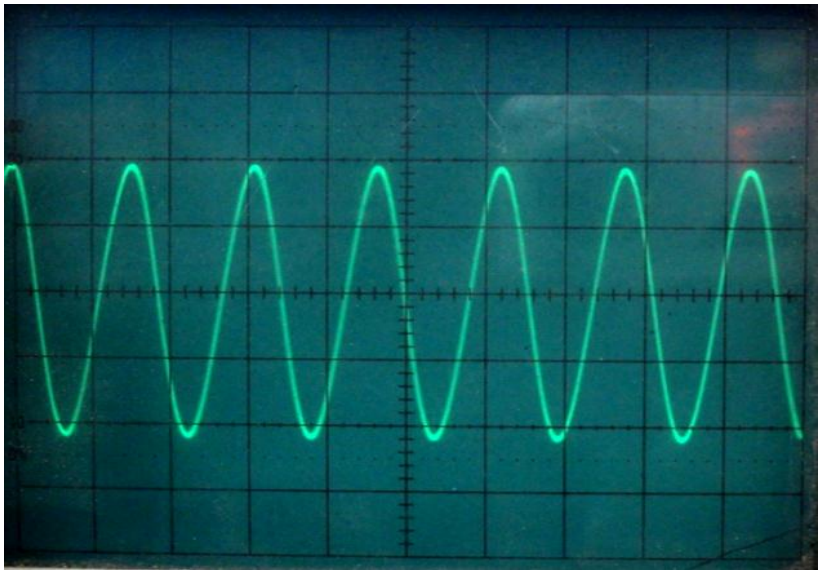

Scale: X-axis 5 µs/div and Y-axis 1 V/div.
Fig. 8.5 Output waveform of the proposed circuit shown in Fig. 4.4 (c)

The passive components, R_1 = 1 kΩ, R_3 = 150 Ω, R_7 = 15 Ω, C_5 = 1 nF and C_6 = 10 nF are used to design the proposed oscillator circuit shown in Fig. 4.4 (c). The corresponding output waveform on the oscilloscope for the proposed oscillator circuit shown in Fig. 4.4 (c) is given in Fig. 8.5. The experimental oscillation frequency of the oscillator circuit is 125 kHz, which is close to the theoretical value of 129.3 kHz.

The proposed circuit shown in Fig. 4.4 (d) is constructed with the passive components R_2 = 500 Ω, R_3 = 12 kΩ, R_5 = 400 Ω, R_7 = 2 kΩ, C_4 = 10 nF and C_6 = 1 nF on a laboratory breadboard. Fig. 8.6 describes the output waveform of the oscillator circuit with a frequency of 23.8 kHz, whereas, the theoretical oscillation frequency is 27.02 kHz. The tunability of the proposed circuit is checked with the passive components R_2 = 500 Ω, R_3 = 12 kΩ, R_5 = 400 Ω, C_4 = 10 nF, C_6 = 1 nF and R_7 is varied from 1 kΩ to 10 kΩ. The variation of oscillation frequency with respect to the resistor R_7 is shown in Fig. 8.7. For producing the oscillations in the proposed oscillator circuit as in Fig. 4.4 (e), the passive components R_2 = 1 kΩ, R_4 = 60 Ω, R_7 = 50 Ω, C_6 = 10 nF and C_3 = 100 nF are connected to the prototype OTRA circuit on a laboratory breadboard.

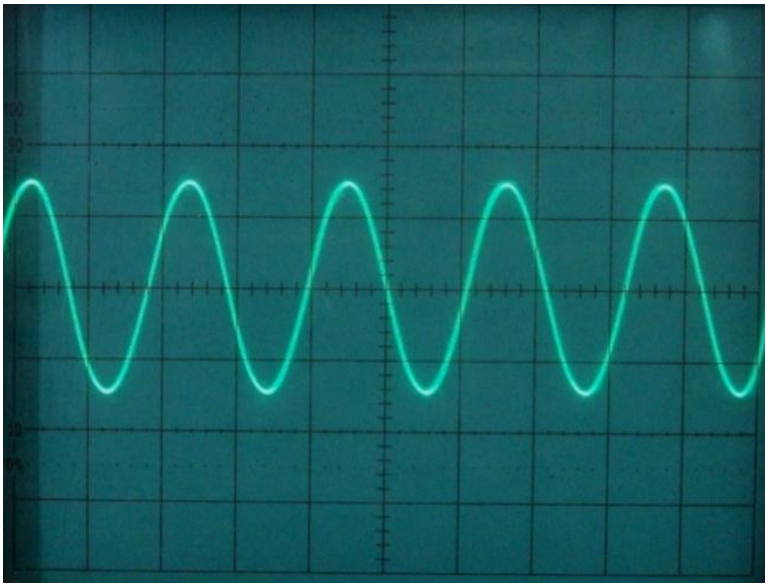

Scale: X-axis 50 µs/div and Y-axis 1 V/div
Fig. 8.6 Output waveform of the proposed circuit in Fig. 4.4 (d)

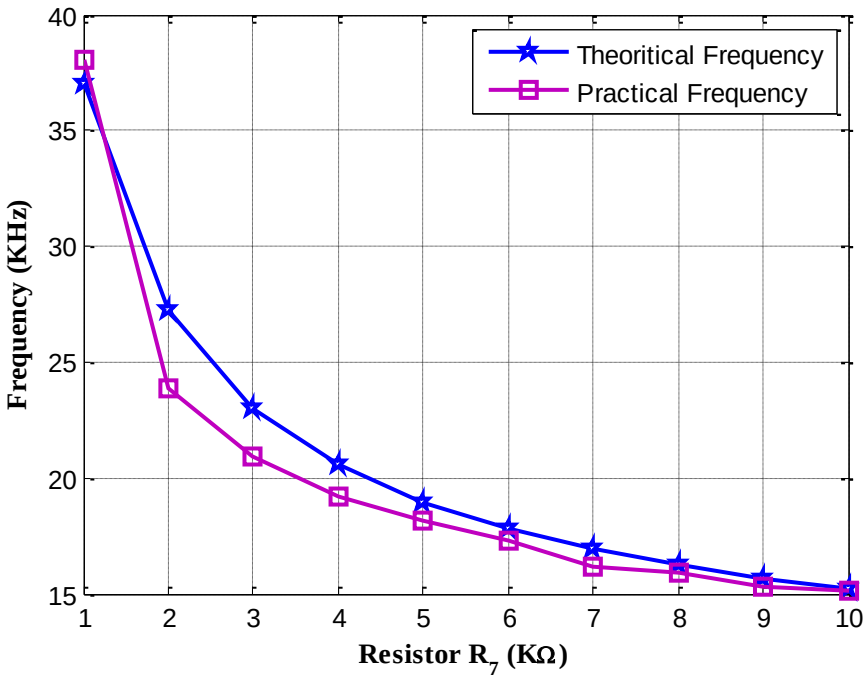

Fig. 8.7 Tunability of the proposed circuit in Fig. 4.4 (d) with respect to the resistor R_7

The experimental output waveform of the proposed circuit is given in Fig. 8.8 with a frequency of 35.7 kHz, whereas the theoretical oscillation frequency was calculated as 30.2 kHz. The variation of oscillation frequency with respect to the passive component connected to the circuit is shown in Fig. 8.9. For generating the variation of oscillation frequency figure, the passive components R_1 = 1 kΩ, R_4 = 60 Ω, C_6 = 10 nF and C_3 = 100 nF have been used and R_7 is varied from 700 Ω to 10 kΩ.

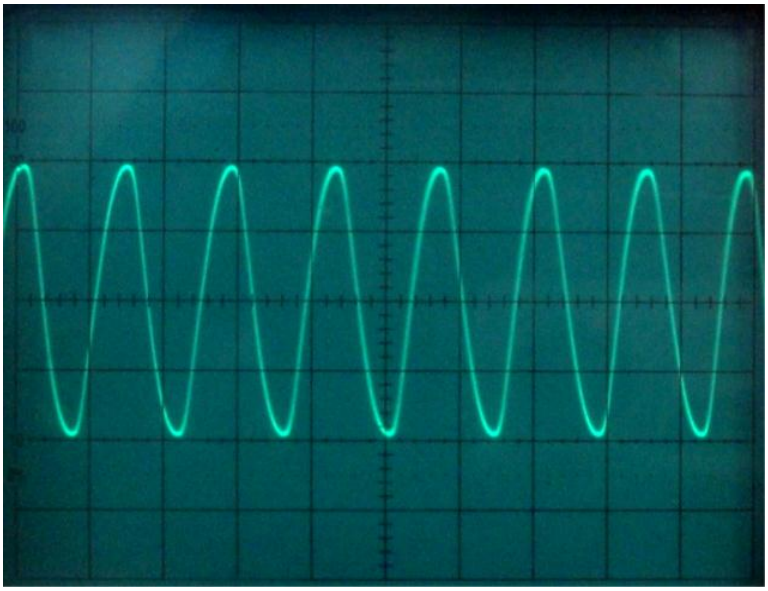

Scale: X-axis 20 µs/div and Y-axis 1 V/div.
Fig. 8.8 Output waveform of the proposed circuit in Fig. 4.4 (e)

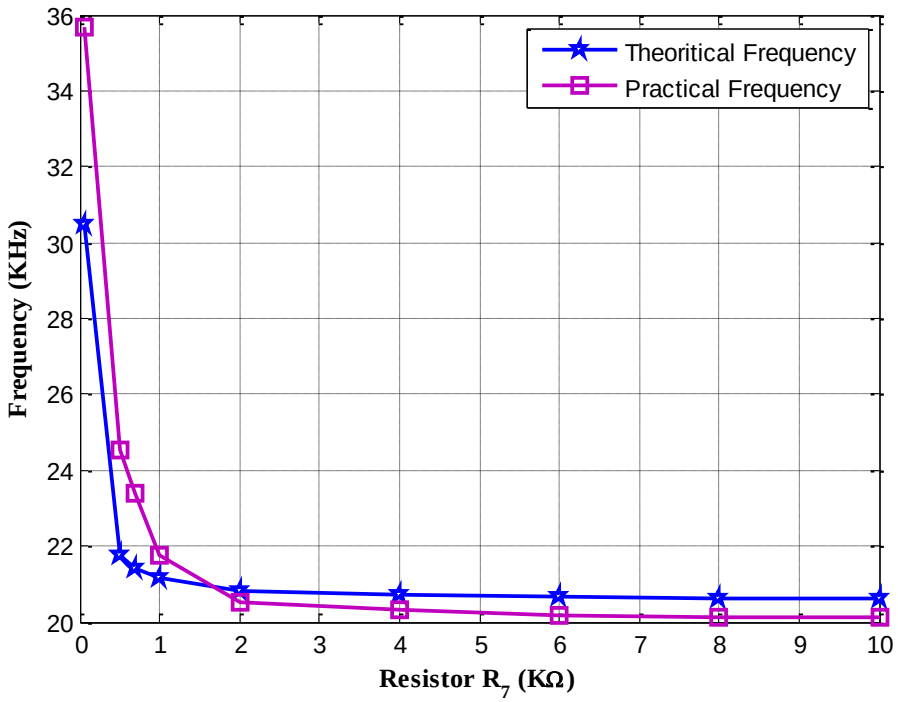

Fig. 8.9 Tunability of the proposed circuit in Fig. 4.4 (e) with respect to the resistor R_7

The Fig. 8.1 is connected with the external passive components C_2 = 10 nF, C_4 = 100 nF, R_3 = 100 Ω, R_5 = 1 kΩ, R_6 = 7 kΩ and R_7 = 200 Ω on a laboratory breadboard for generating the oscillations in the proposed circuit shown in Fig. 4.4 (f). The experimental output waveform of proposed circuit is given in Fig. 8.10 with a frequency of 18.18 kHz which is close to the theoretical result of 18.6 kHz.

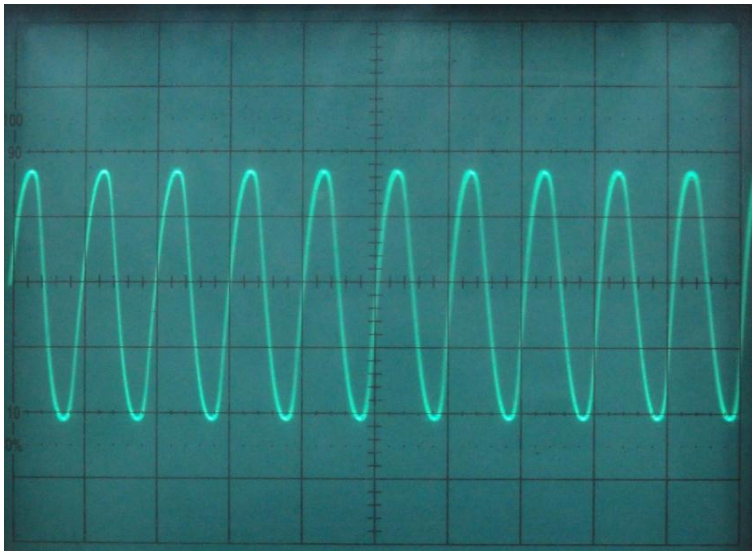

Scale: X-axis 50 µs /div and Y-axis 2 V/div

Fig. 8.10 Experimental output wave form of the proposed circuit in Fig. 4.4 (f)

For generating the oscillations in the proposed circuit shown in Fig. 4.4 (g), the passive component values are chosen to be R_3 = 1 kΩ, R_6 = 1 kΩ, R_7 = 5 kΩ, C_2 = 100 nF and C_4 = 100 nF. Figure 8.11 represents the experimental output waveform of the proposed circuit with a frequency of 19 kHz which is close to the theoretical result of 20 kHz.

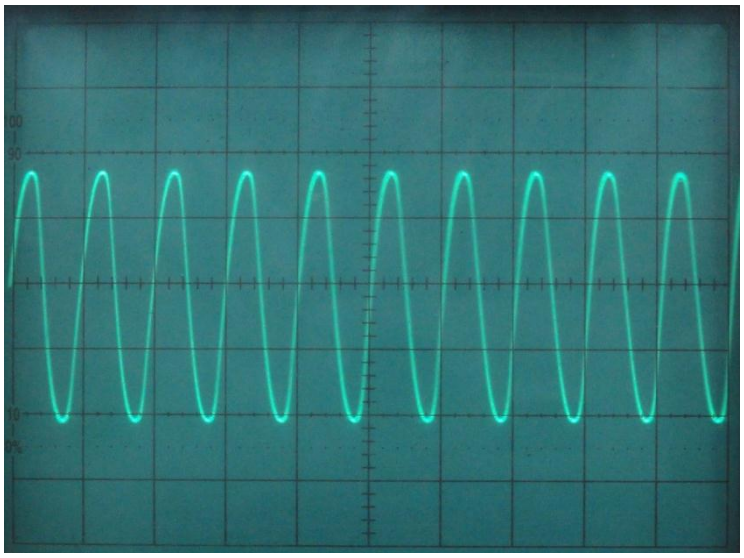

Scale: X-axis 50 µs /div and Y-axis 2 V/div

Fig. 8.11 Experimental output wave form of the proposed circuit in Fig. 4.4 (g)

The passive component values C_1 = 100 nF, C_3 = 100 nF, R_2 = 50 Ω and R_4 = 500 Ω are used for the proposed circuit shown in Fig. 4.4 (h) to generate oscillations.

The experimental output waveform of the proposed circuit in Fig. 4.4 (h) is given in Fig. 8.12.

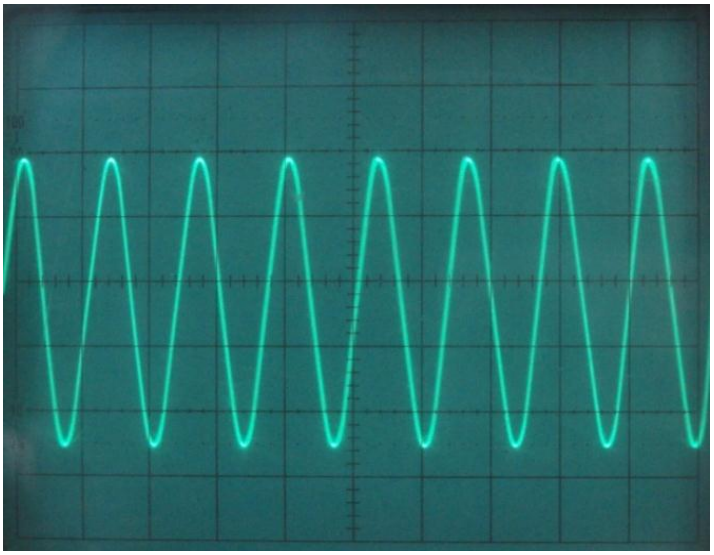

Scale: X-axis 50 µs/div and Y-axis 2 V/div
Fig. 8.12 Experimental output wave form of the proposed circuit in Fig. 4.4 (h)

Likewise, the passive components values C_1 = 10 nF, C_2 = 100 nF, R_3 = 100 Ω and R_5 = 5 kΩ are used on a laboratory breadboard for generating the oscillations in the proposed circuit shown in Fig. 4.4 (i). The experimental output waveform of the proposed circuit in Fig. 4.4 (h) is given in Fig. 8.13.

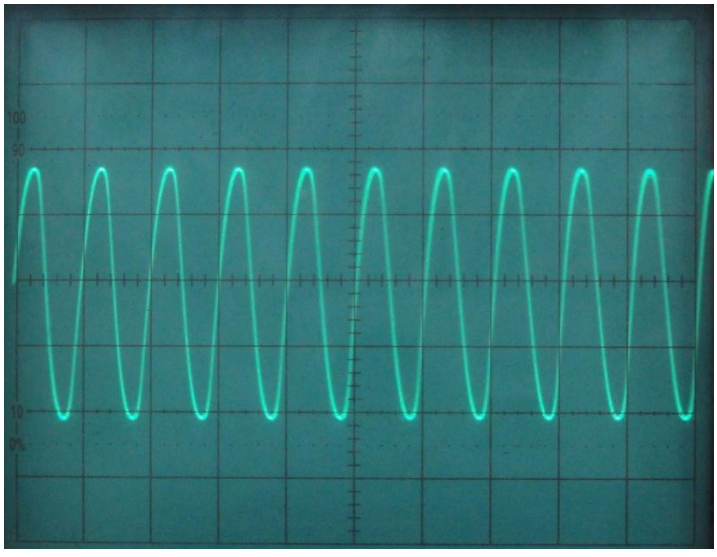

Scale: X-axis 50 µs /div and Y-axis 2 V/div
Fig. 8.13 Experimental output wave form of the proposed circuit in Fig. 4.4 (i)

The following passive components values are chosen for the proposed circuit in Fig. 4.5 (a), R_1 = 100 Ω, R_2 = 1.2 kΩ, R_3 = 600 Ω, R_4 = 5.5 kΩ, C_2 = 10 nF and C_3 =

100 nF. Figure 8.14 represents the experimental output waveform of the proposed circuit in Fig. 4.5 (a) with a frequency of 10.3 kHz, which is close to the theoretical value of 10 kHz.

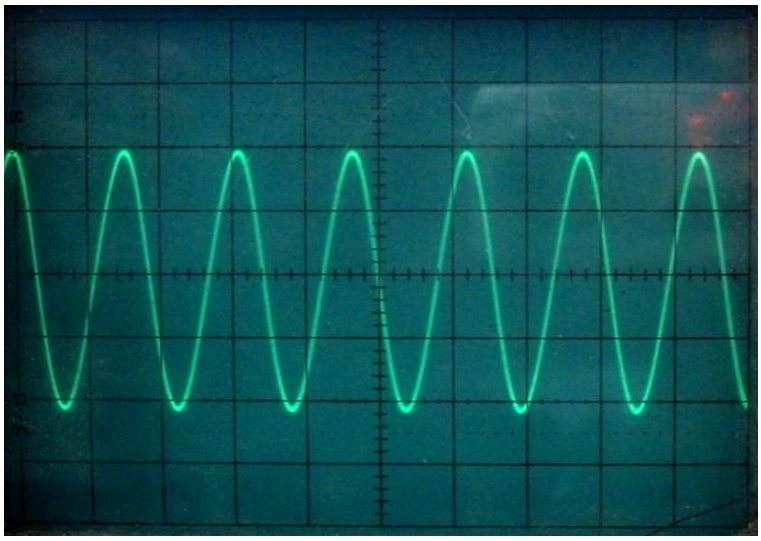

Scale: X-axis 50 μs/div and Y-axis 1 V/div.
Fig. 8.14 Experimental output waveform of the proposed circuit in Fig. 4.5 (a).

Similarly, the proposed circuit shown in Fig. 4.5 (b) is connected on a laboratory breadboard with the following external passive components R_1 = 100 Ω, R_2 = 1.2 kΩ, R_3 = 600 Ω, R_4 = 5.5 kΩ, C_2 = 10 nF and C_3 = 100 nF. The experimental output waveform is depicted in Fig. 8.15.

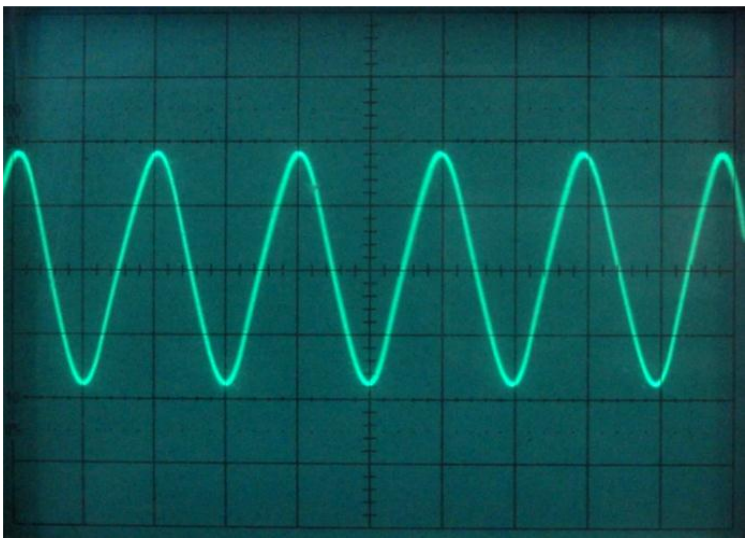

Scale: X-axis 20 μs/div and Y-axis 1 V/div.
Fig. 8.15 Experimental output waveform of the proposed circuit in Fig. 4.5 (b)

The comparative analysis of the proposed oscillator and quadrature oscillator circuits shown in Fig. 4.4 (a) and Fig. 4.6 with the existing oscillator circuits in the literature is shown in the Table 8.1.

TABLE 8.1 Comparison of the proposed circuit in Fig. 4.4 (a) and 4.6 with the conventional sinusoidal oscillators in the literature

Oscillator circuits	Number of active components	Total number of resistors	Total number of capacitors	Total number of components	Supply voltage (V)	Power consumption (mW)
[21]	2 CCII	2	2	6	± 9	278.4
[22]	2 CCII	3	4	9	± 15	≈ 600
[30] Fig. 4	2 CCII	4	3	9	± 9	520
[29] Fig. 1 (a)	3 CFOA	4	2	9	± 12	648
[50] Fig. 4	2 OTRA	4	2	8	± 5	250.8
[50] Fig. 5 (a) & 5 (b)	2 OTRA	4	2	8	± 5	250.2
[51]	1 OTRA	3	2	6	± 5	114.2
[52] Fig. 4 (a)	1 OTRA	2	2	5	± 5	106.3
Proposed circuit in Fig. 4.4 (a)	1 OTRA	2	2	5	± 5	106.2
Proposed circuit in Fig. 4.6	2 OTRA	4	2	8	± 5	250.4

8.3 QUADRATURE SINUSOIDAL OSCILLATORS

8.3.1 EXPERIMENTAL RESULTS

For generating the oscillations of the proposed circuits shown in Fig. 4.6 and 4.7 on a laboratory breadboard, the OTRA equivalent circuit shown in Fig. 8.1 is connected with external passive components. The quadrature oscillator circuit shown in Fig. 4.6 is connected with the passive components C_2 = 10 nF, C_4 = 100 nF, R_3 =

100 Ω, R_5 = 1 kΩ, R_4 = 7 kΩ and R_1 = 200 Ω to generate the oscillations with 90° phase shift. The corresponding output waveforms of V_{01} and V_{02} on oscilloscope screen are shown in Fig. 8.16.

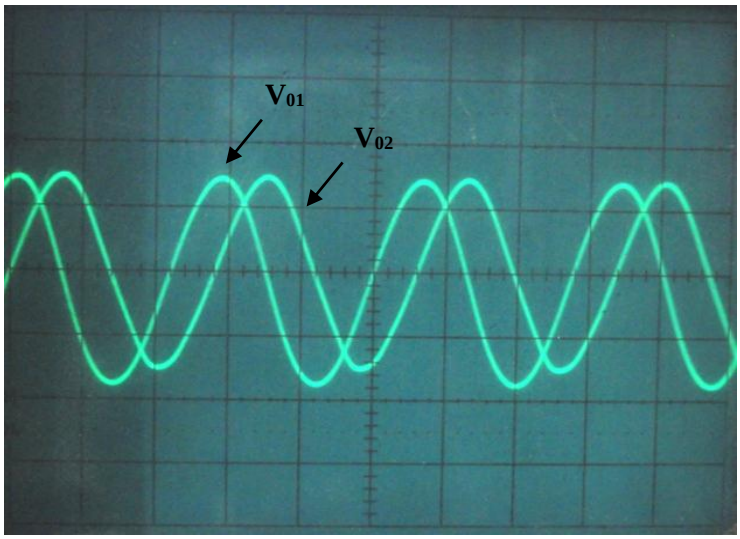

Scale: X-axis 20 µs /div and Y-axis 1 V/div

Fig. 8.16 Experimental output waveform for the proposed circuit in Fig. 4.6

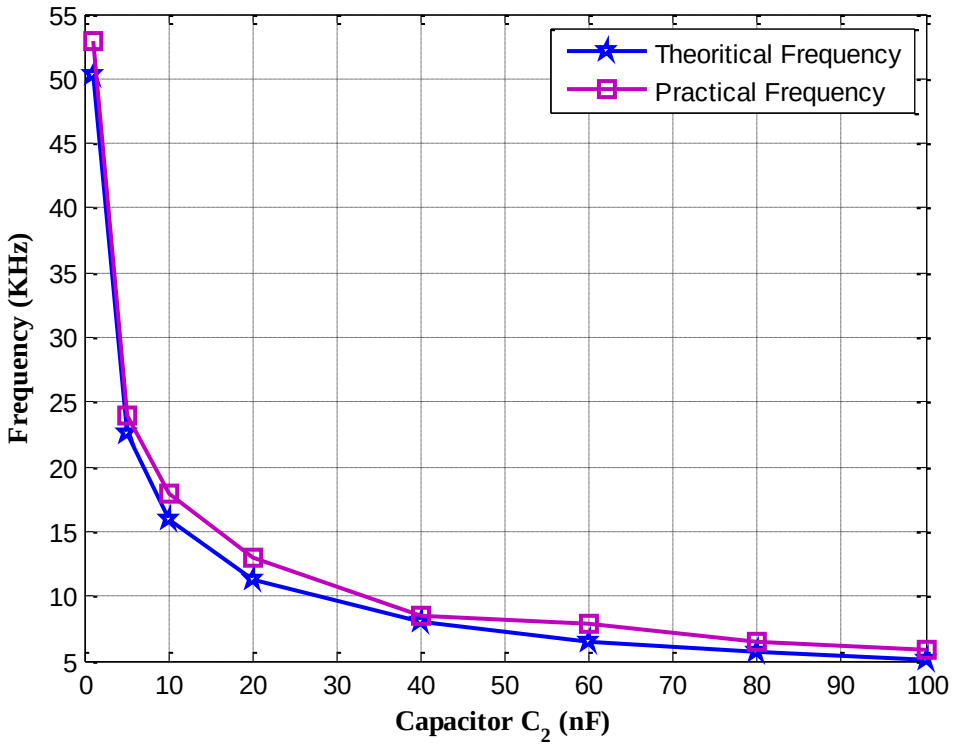

Fig. 8.17 Tunability of the proposed circuit in Fig. 4.6 with respect to the capacitor C_2

The variation of oscillation frequency with respect to the passive component C_2 is shown in Fig. 8.17. For this figure, the passive components C_4 = 100 nF, R_3 = 100 Ω,

R_5 = 1 kΩ, R_4 = 7 kΩ and R_1 = 200 are used and C_2 is varied form 1 nF to 100 nF. The lissajous curves of the output voltages V_{01} verses V_{02} is shown in Fig. 8.18.

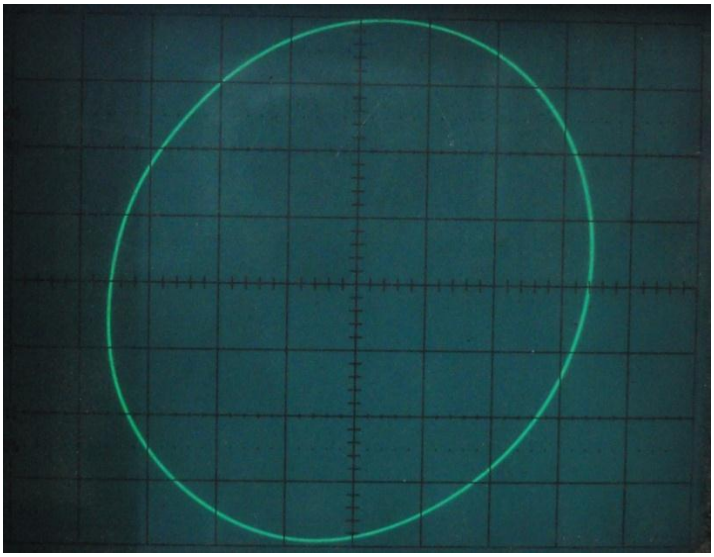

Fig. 8.18 The voltages V_{01} versus V_{02} of the proposed quadrature oscillator on oscilloscope

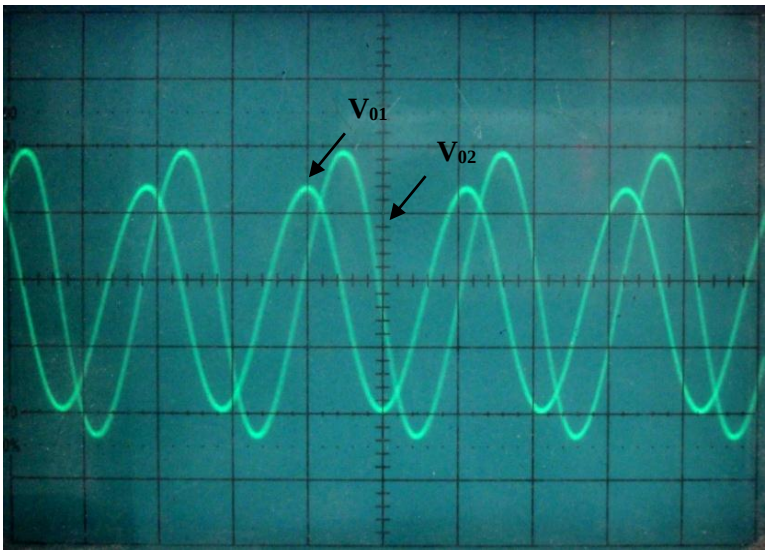

Scale: X-axis 20 μs/div and Y-axis 1 V/div
Fig. 8.19 Experimental output waveform of the proposed circuit in Fig. 4.7

Similarly, the proposed circuit shown in Fig. 4.7 is connected with the passive components R_1 = 9 kΩ, R_2 = 500 Ω, R_3 = 1 kΩ, R_5 = 100 Ω, C_1 = 10 nF and C_4 = 10 nF on a laboratory breadboard for waveform generation. The output waveforms at the output terminals V_{01} and V_{02} of the OTRAs in Fig 4.7 is shown in Fig. 8.19. The variation of oscillation frequency with respect to the capacitor C_1 is shown in Fig. 8.20. For this figure, the passive components R_1 = 9 kΩ , R_2 = 500 Ω, R_3 = 1 kΩ, R_5 = 100 Ω,

and C_4 = 10 nF have been used and C_1 is varied from 1 nF to 100 nF. The lissajous curves between the output voltages V_{01} verses V_{02} is shown in Fig. 8.21.

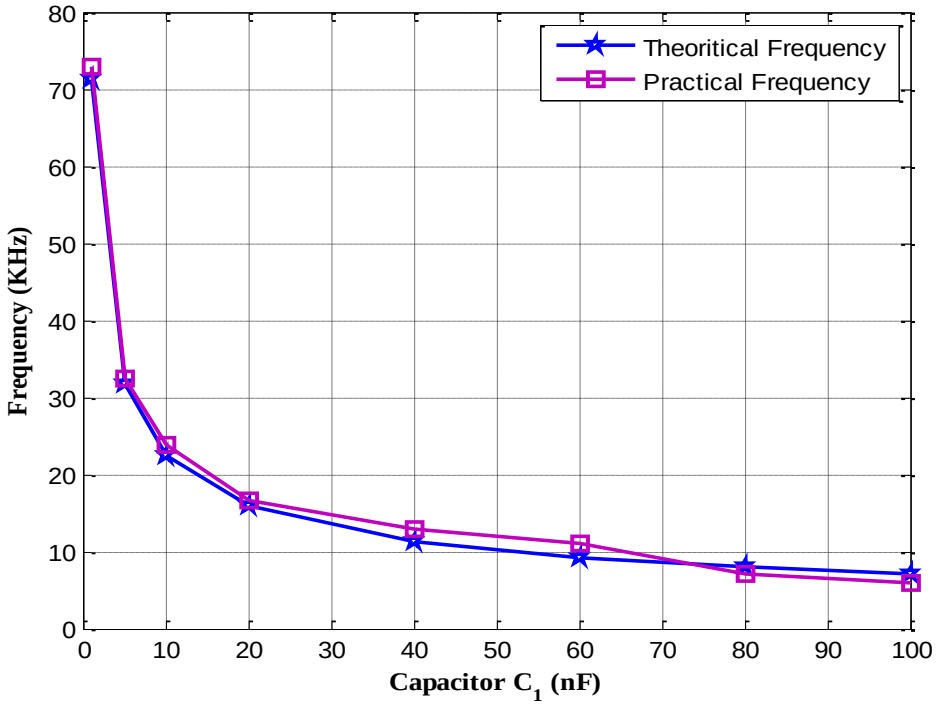

Fig. 8.20 Tunability of the proposed circuit in Fig. 4.6 with respect to the capacitor C_1

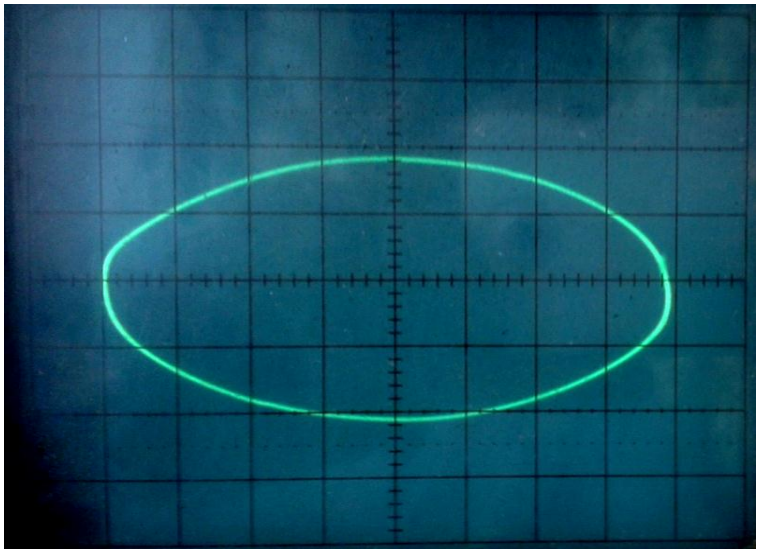

Fig. 8.21 The voltage V_{01} versus V_{02} of the proposed quadrature oscillator on oscilloscope

8.4 SQUARE WAVEFORM GENERATORS

8.4.1 EXPERIMENTAL RESULTS

For the proposed square waveform generator circuit shown in Fig. 4.8 (a), the required time period is chosen first. Then, suitable values of passive components (R_1, R_2 and C) are derived from the time period or frequency equations (5.46) or (5.47). For higher sensitivity of the time period with respect to the resistor, the resistor R_2 is chosen to be less than 2 kΩ. For example, if the required time period is 7.19 µs, then R_1, R_2 and C values are chosen to be 15 kΩ, 1.5 kΩ and 1 nF. The proposed circuit shown in Fig. 4.8 (a) is connected on a laboratory breadboard with the help of the OTRA equivalent model shown in Fig. 8.1 and the selected passive components. The experimental output waveform of the proposed circuit shown in Fig. 4.8 (a) is given in Fig. 8.22 with a time period of 7.02 µs.

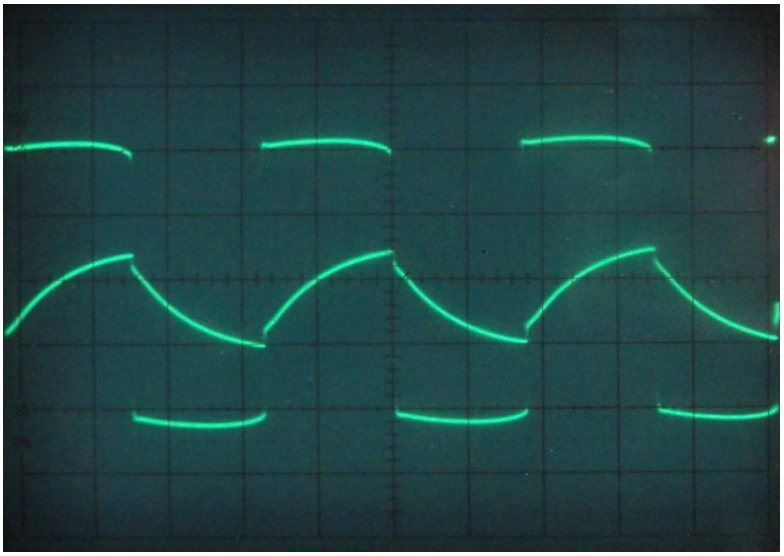

Scale: X-axis 2 µs/div and Y-axis 2 V/div.

Fig. 8.22 Output waveform with almost equal and fixed duty cycles ($T_{ON} = T_{OFF}$)

Similarly, in the case of second proposed circuit shown in Fig. 4.8 (b), the suitable passive component values will be obtained from the equation (5.53) or (5.54) for a selected time period. If the required time period is 0.32 ms with 60 % on-duty and 40 % off-duty cycles. The resistors and capacitor values chosen to set the required time period are R_2 = 1.5 kΩ R_{11} = 1.5 kΩ, R_{12} = 5 kΩ and C = 0.1 nF. The capacitor C is slightly increased to set the required time period. The resistor R_{11} and R_{12} values will be reversed to set the 40 % on-duty and 60 % off-duty cycles.

The output waveform with 60 % on-duty and 40 % off-duty cycle for the second proposed circuit is shown in Fig. 8.23 (a). Likewise, the passive components R_2 = 1.5 kΩ, R_{11} = 5 kΩ, R_{12} = 1.5 kΩ and C = 0.1 nF are selected to get the 40 % on-duty and 60 % off-duty cycles with the proposed circuit shown in Fig. 4.8 (b).

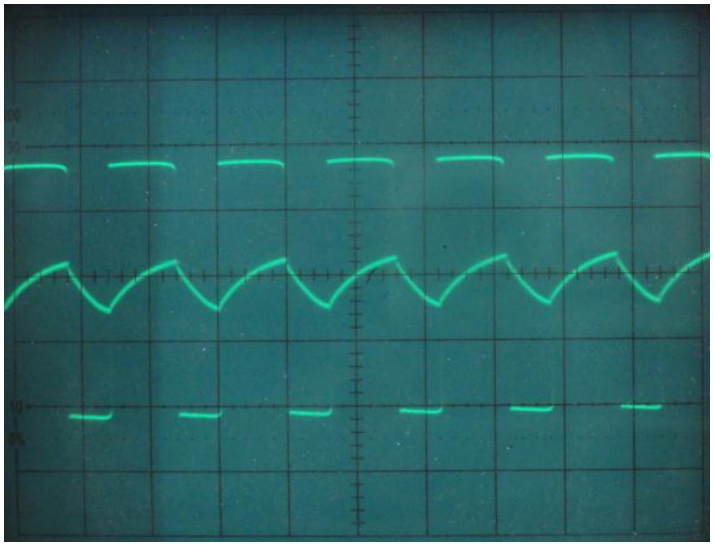

Scale: X-axis 0.2 ms/div and Y-axis 5 V/div.
(a) Output waveform with variable on-duty cycle ($T_{ON} > T_{OFF}$)

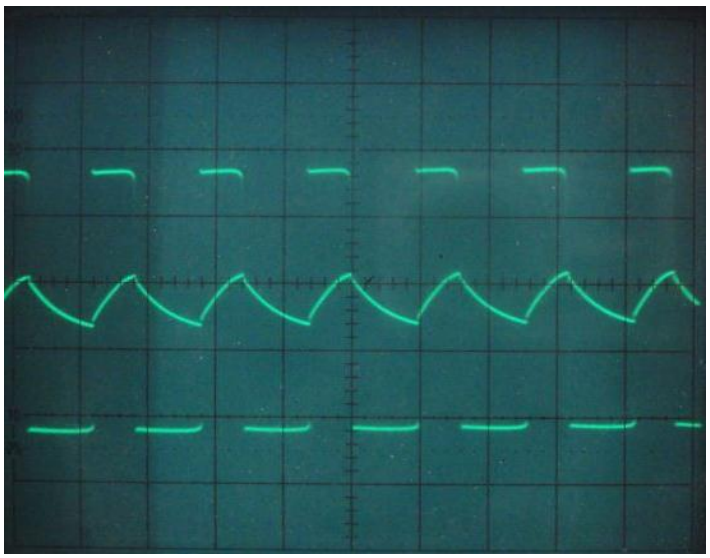

Scale: X-axis 0.2 ms/div and Y-axis 5 V/div.
(b) Output waveform with variable off-duty cycle ($T_{ON} < T_{OFF}$)

Fig. 8.23 Experimental output waveforms of the second proposed circuit

The experimental output waveform with 40% on-duty and 60% off-duty cycle is shown in Fig. 8.23 (b). Several experiments are performed on a laboratory breadboard to test the tunability of the proposed circuits shown in Fig. 4.8 (a) and (b) against the passive components R_1, R_2 and C. The results are presented in Figs. 8.24 - 8.26 for the

proposed circuit configuration shown in Fig. 4.8 (a). For all measurements on tunability, the supply voltage of ± 5 V is used. Figures 8.24, 8.25 and 8.26 denote the time period variation against the passive components R_1, R_2 and C.

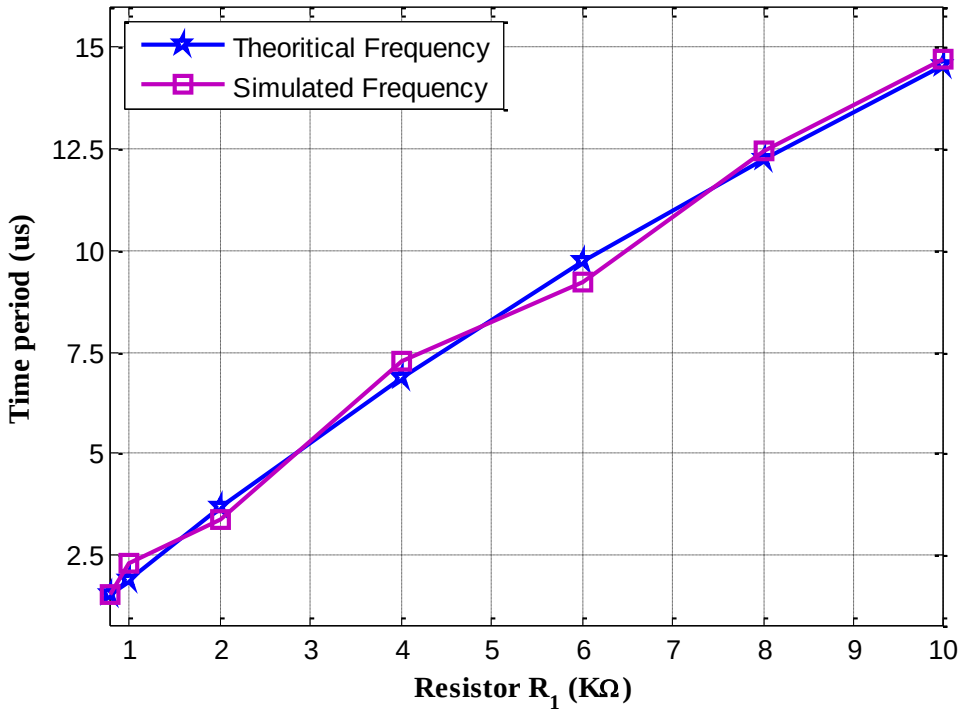

Fig. 8.24 Variation of time period against resistor R_1

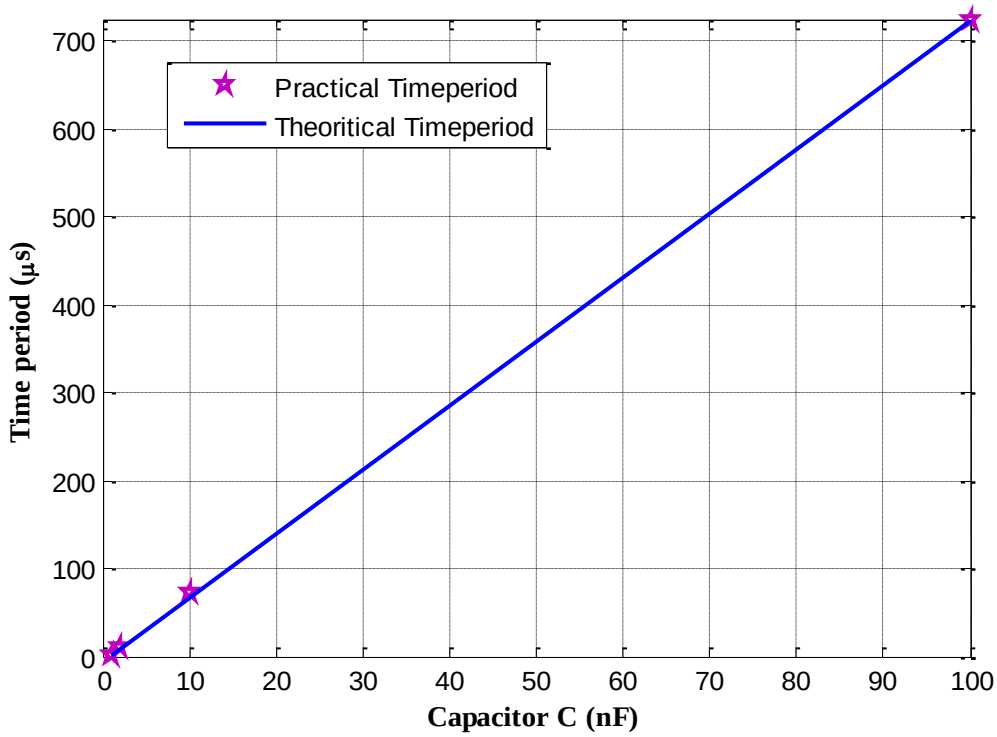

Fig. 8.25 Tunability against capacitor C

TABLE 8.2. Comparison of the proposed circuit in Fig. 4.8 (a) with the conventional square-wave generators in the literature

Square wave designs	Propsed design in Fig. 4.8(a)	Hou *et al.*2005 [45]	Chung *et al.*2005 [27]	Del re *et al.* 2007 [26]	Andrea *et al.* 2011 [25]	Pal *et al.* 2009 [18]	Srinivasulu 2011 [19]	Abuelmatti et al. 1998 [24]	Haque et al. 2008 [28]
No. of active components	1 OTRA	1 OTRA	3 OTA	1 CCII+	2 CCII+	2 CCII+	3 CCII+	1 CFOA	2 CFOA
No. of passive components	3 (1 Capacitor and 2 Resistors)	3 (1 Capacitor and 2 Resistors)	3 (1 Capacitor and 2 Resistors)	4 (1 Capacitor and 3 Resistors)	6 (1 Capacitor and 5 Resistors)	4 (1 Capacitor and 3 Resistors)	7 (1 Capacitor and 6 Resistors)	4 (1 Capacitor and 3 resistors)	5 (1 Capacitor and 4 Resistors)
No. of compo-nents	4	4	6	5	8	6	10	5	7
Maximum frequency range	3.33 MHz	12.5 MHz	16 kHz	2 kHz	737 kHz	260 kHz	574 kHz	71 kHz	60 MHz
Supply voltage	± 5 V	± 15 V	± 5 V	1.5 V (Integrate solution)	±15 V	± 5 V to ±15 V	± 6 V	Not available	± 5 V
Power consumption	182 mW	315 mW	> 1.8 W	750 µW (Integrate solution)	400 mW	384 mW	240 mW	Not available	Not available

For the tunability of resistor R_1, the selected passive component values are R_2 = 12 kΩ, C = 1 nF and R_1 is varied from 800 Ω to 10 kΩ. A linear variation of time period was exhibited by the circuit and it is presented in the form of plot in Fig. 8.24. Similarly, for the capacitor C, the selected parameter values are resistors R_1 = 15 kΩ and R_2 = 1.5 kΩ. The capacitor C is varied from 1 nF to 100 nF. The practical and theoretical time period variation against the capacitor C is plotted in Fig. 8.25.

Likewise, for the resistor R_2, the circuit is built with resistor R_1 = 15 kΩ, capacitor C = 1 nF and R_2 is varied from 200 Ω to 3 kΩ. The result is plotted in Fig. 8.26. From Figs. 8.24, 8.25 and 8.26, the variation of time period with respect to the passive components is linear. The comparative analysis of the proposed circuit shown in Fig. 4.8 (a) with the existing square wave generator circuits in the literature is shown in the Table 8.2.

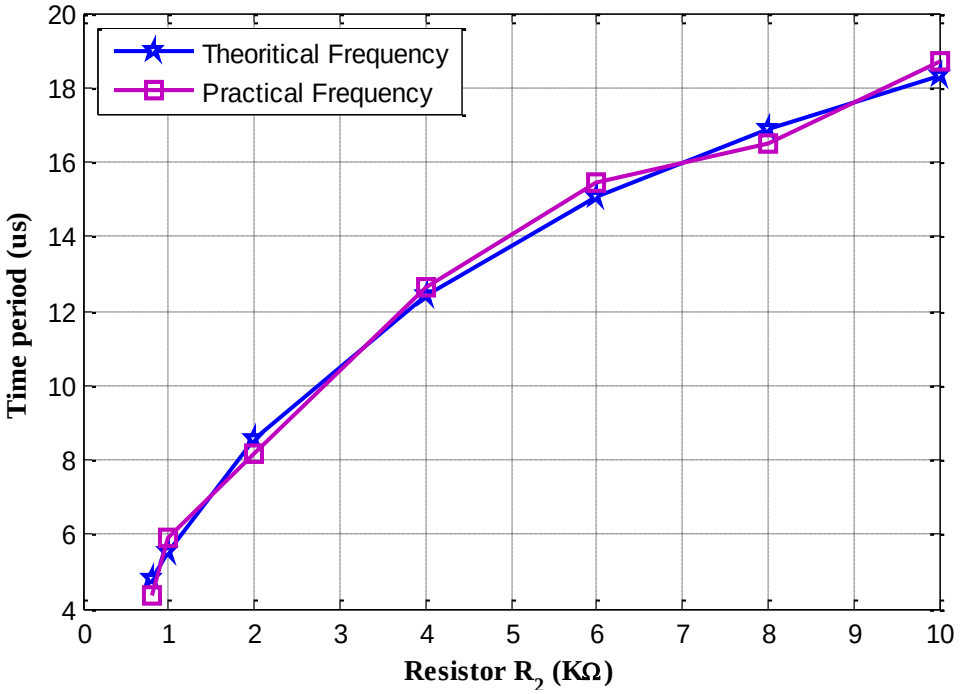

Fig. 8.26 Tunability against resistor R_2

The proposed circuits in Figs. 4.8 (a) and (b) will generate the waveforms independent of the resistor values and it exhibits more linear curve than the conventional OTRA square waveform generator circuits. The proposed circuits can generate the oscillations up to 3.33 MHz.

8.5 SUMMARY

In this chapter, experimental results are presented to validate the simulation analysis and theoretical analysis of the proposed circuits. All the proposed circuits are designed on a laboratory breadboard and corresponding output waveforms are presented in this chapter. The variation of oscillation frequency with respect to the passive components connected to the circuits is also presented for some circuits. For all the proposed circuits, experimental frequencies are matched with the simulated frequencies and the theoretically calculated frequencies.